

Plasticity and not adaptation is the primary source of temperature-mediated variation in flowering phenology in North America

Tadeo Ramirez-Parada (✉ tadeo@ucsb.edu)

UC Santa Barbara

Isaac Park

UC Santa Barbara

Sydne Record

University of Maine

Charles Davis

Harvard University <https://orcid.org/0000-0001-8747-1101>

Aaron Ellison

Harvard University

Susan Mazer

UC Santa Barbara

Article

Keywords:

Posted Date: July 7th, 2023

DOI: <https://doi.org/10.21203/rs.3.rs-3131821/v1>

License: © ⓘ This work is licensed under a Creative Commons Attribution 4.0 International License.

[Read Full License](#)

Additional Declarations: There is **NO** Competing Interest.

Version of Record: A version of this preprint was published at Nature Ecology & Evolution on January 11th, 2024. See the published version at <https://doi.org/10.1038/s41559-023-02304-5>.

Abstract

Phenology varies widely over space and time because of its sensitivity to climate. However, whether phenological variation is primarily generated by rapid organismal responses (i.e., plasticity) or local adaptation remains unresolved. Here, we used 1,038,027 herbarium specimens representing 1,605 species to measure flowering time sensitivity to temperature over time (S_{time}) and space (S_{space}). By comparing these estimates, we inferred how adaptation and plasticity historically influenced phenology along temperature gradients and how their contributions vary among species with different phenology and native climates, and among ecoregions differing in species composition. S_{space} and S_{time} were highly positively correlated ($r = 0.87$), of similar magnitude, and more frequently consistent with plasticity than adaptation. Apparent plasticity and adaptation generated earlier flowering in spring, limited responsiveness in summer, and delayed flowering in fall in response to temperature increases. Nonetheless, ecoregions differed in the relative contributions of adaptation and plasticity, from consistently greater importance of plasticity (e.g., Southeastern USA Plains) to their nearly equal importance throughout the season (e.g., Western Sierra Madre Piedmont). Our results support the hypothesis that plasticity is the primary driver of flowering time variation along climatic gradients, with local adaptation having a widespread but comparatively limited role.

Introduction

The timing of life-cycle events ('phenology') determines the environmental conditions that organisms encounter throughout development and often mediates their fitness¹. Phenology usually is cued by seasonally and interannually variable climatic factors—such as temperature—that enable individuals to adjust growth and reproduction plastically in response to fluctuating environmental conditions^{1,2}. Phenology also varies intraspecifically as a result of evolutionary adaptation to local environments, which may select for different mean phenological timings among or within populations in space and time^{3–6}. Although both plasticity and adaptation alter phenology, their relative contributions rarely have been measured within the same system largely because doing so requires experiments or spatiotemporally extensive genetic sampling^{7–9} (but see ⁶). Accordingly, most studies have highlighted either plasticity or adaptation as mechanisms of phenological variation due to environmental change⁷ but their relative importance across species and ecological contexts remains unresolved. Elucidating the degree to which species have phenologically responded to historical climatic variation through plasticity or adaptation could provide important context for predicting whether organismal responses may be sufficient—or evolutionary change necessary—to maintain development and climate synchronized in a warming world⁸.

Phillimore et al.⁹ proposed that the contributions of plasticity and local adaptation to spatial variation in phenology within a species can be estimated from the difference between the slopes of spatial and temporal phenology-climate relationships. This proposition rests on several observations. The effects of interannual climatic variation on phenology generally reflect plastic responses, especially among long-

lived species less liable to experience microevolutionary changes from year to year¹⁰. Similarly, phenological variation over space can be caused by phenotypic plasticity where, for example, growing-degree day (GDD) thresholds that trigger life-cycle events occur on different dates across sites¹¹. However, among populations, local adaptation also can generate phenological variation along climatic gradients^{12,13}. Therefore, assuming no confounding factors, and absent significant variation in phenological plasticity within and among populations, spatial phenology-climate relationships should reflect the joint effects of plasticity and adaptation¹⁴.

Given these observations and assumptions, plasticity and adaptation can generate four empirical patterns of sensitivity to temporal and spatial climatic variation (Fig. 1). First, if a species does not show phenological plasticity but population-level phenological means are locally adapted across a climatic gradient, we should observe negligible sensitivity to temporal climatic variation (i.e., no plasticity) and a biologically significant difference between the slopes of the temporal and spatial relationships (attributable to adaptation) (Figs. 1a,b). Alternatively, a phenologically plastic species whose populations are not locally adapted along the gradient should show biologically significant sensitivity to interannual climatic variation and no differences between temporal and spatial slopes (Figs. 1c,d), implying that variation along the gradient can be attributed to plastic responses. Finally, when both adaptation and plasticity drive phenological variation along the climate gradient, the resulting empirical pattern should depend on the relative direction of plastic and adaptive responses. Specifically, we should observe a greater spatial than temporal sensitivity when adaptation operates in the same direction as plasticity (i.e., “co-gradient adaptation”; Fig. 1e,f), and a lesser spatial sensitivity or one of opposite direction to the temporal response when adaptation operates in the opposite direction (i.e., “counter-gradient adaptation”; Fig. 1g,h; see Fig. S1 for examples of species representing each of these patterns)^{15,16}.

Phenological sensitivity to temperature often varies among species occurring in different regions or that initiate phenological events at different times throughout the growing season^{17–24}. However, comparisons of phenological sensitivity to climate over space and time—which are necessary to evaluate the apparent contributions of plasticity and adaptation across ecological contexts (Fig. 1)—require spatiotemporally extensive datasets and therefore remain rare. Herbaria provide abundant and increasingly available data to conduct these analyses at unprecedented taxonomic, temporal, and spatial scales^{21,25–30}. However, few studies have separately estimated sensitivity to spatial versus temporal climate variation using specimens (but see^{28,31–34}), and none have leveraged their unique scope to determine the ecological contexts in which plasticity or adaptation might contribute more strongly to spatial variation in phenology.

Here, we analyzed a dataset of over a million flowering specimens from 1,605 species across the continental United States to compare phenological sensitivities to spatial and temporal variation in temperature (S_{space} and S_{time} , respectively). For each species, we assessed whether its empirical sensitivity patterns were consistent with the effects of plasticity, adaptation, or both along temperature gradients (Fig. 1). Additionally, we evaluated how apparent temperature-related plasticity and adaptation

of flowering time varied among species with different native climates, phenological niches, and occurring within different regional floras. Together, our analyses identified ecological contexts in which plasticity or adaptation appear to have most strongly influenced spatial phenological variation, providing the most taxonomically and geographically extensive assessment of temperature-mediated variation in flowering time among North American angiosperms conducted to date.

Results

Plasticity vs. adaptation as causes of flowering time variation along temperature gradients

S_{space} and S_{time} of most species differed from 0 with at least 95% probability (93% and 79% of species, respectively). S_{space} and S_{time} agreed in direction for 94% of species, and estimates of both S_{time} and S_{space} were negative for most taxa (89% and 91%, respectively), indicating earlier flowering across increasingly warmer locations and in warmer-than-average years (Fig. 2a).

Both apparent plasticity and adaptation were associated with clinal variation in flowering time along temperature gradients, with plasticity playing a predominant role among species. S_{space} and S_{time} were highly positively correlated, and their magnitude tended to correspond 1-to-1 for many species (Fig. 2b). Therefore, flowering shifts in warmer-than-average years typically had similar direction and magnitude (in days/°C) as those observed across increasingly warmer locations, consistent with a scenario of plasticity as the cause of phenological variation along the spatial temperature gradients (Figs. 1c,d; Table 1).

More species showed sensitivity patterns consistent with plasticity than with adaptation (79% versus 45%, respectively) (see classification scheme in Table 1). Apparent plasticity explained approximately 52% of the variance in flowering time clines along temperature gradients among species (i.e., R^2 of the 1-to-1 line of S_{time} vs. $S_{\text{space}} = 0.52$; Fig. 2b). Consistently, a plurality of species (41%) showed sensitivity patterns consistent with plasticity as the sole driver of phenological variation across gradients. In contrast, only 7% of species showed sensitivity patterns consistent solely with adaptation (see Figs. 1a,b). Rather, most species showing apparent local adaptation concurrently showed evidence of plasticity (38%). Among these, a greater proportion showed flowering advances (27%) than flowering delays (10%) resulting from apparent adaptation. 14% of species showed patterns that were neither consistent with temperature-related plasticity nor with adaptation. These patterns remained consistent when including only long-lived species in the analyses (whose responses to yearly temperature anomalies are certain to be plastic; Fig. S2).

Plasticity and adaptation across phenological niches, native climates, and ecoregions

Apparent plasticity (S_{time}) varied substantially among species with different phenological niches and across local climates ($R^2 = 0.47$; Fig. 3a, c). Species flowering during late winter and spring tended to show flowering advances in warmer-than-average years. Such advances decreased in magnitude throughout the season, typically reversing to flowering delays during late summer and fall (Fig. 3a,c).

Apparent adaptation ($S_{\text{space}} - S_{\text{time}}$) also varied with phenological niche and native climate ($R^2 = 0.45$, Figs. 3b, d). $S_{\text{space}} - S_{\text{time}}$ varied from negative to positive values throughout the growing season across PC1, indicating a transition from flowering advances to delays attributable to local adaptation (Fig. 3b). Such transition occurred much earlier in cool, thermally seasonal regions (i.e., the low range of PC1). Apparent adaptation also varied throughout the growing season along PC2, except in dry, thermally seasonal regions of the gradient (Fig. 3d).

These patterns were mirrored at the regional level: throughout the season, average apparent plasticity and adaptation among species transitioned from generating flowering advances to generating delays in response to higher temperatures in all sampled ecoregions; this transition invariably occurred during the summer months (R^2 for $S_{\text{time}} = 0.44$; R^2 for $S_{\text{space}} - S_{\text{time}} = 0.35$; Fig. 4). The magnitude of apparent adaptation tended to be lower than that of apparent plasticity throughout the year for all ecoregions, but their difference tended to be lesser among species flowering early or late in the season (Figs. 4a–n). Nonetheless, we detected regional differences in the relative contributions of apparent adaptation and plasticity among species throughout the season. For example, apparent adaptation and plasticity showed similar magnitude within the Western Sierra Madre Piedmont (Fig. 4g). In contrast, mean apparent plasticity was consistently greater than adaptation among species in the Southeastern USA Plains (Fig. 4j). The difference in magnitude between apparent plasticity and adaptation was greatest among early- to mid-summer flowering species in the Western Cordilleras and Cold Deserts (Figs. 4b,c).

Discussion

This study provides evidence that, for North American plants, phenotypic plasticity historically has been the primary mechanism generating flowering time variation along temperature gradients. Nonetheless, apparent adaptation and plasticity jointly generated phenological variation in a large proportion of species. Both apparent plasticity and adaptation consistently generated flowering advances in spring, lesser advances during summer, and flowering delays during early fall, and this pattern is consistent across climates and ecoregions. Whether phenological reaction norms to historical climatic conditions will remain adaptive under future climatic regimes is unclear¹⁰. Nonetheless, these results suggest that plasticity historically has enabled phenology to respond quickly to a wide range of temperature conditions among North American angiosperms, with adaptation frequently playing an important but context-dependent role.

Plasticity is the primary cause of temperature-mediated clinal variation in flowering time—Extensive research has documented phenological plasticity to spatial climatic variation in plants^{35–38} that can result in clinal phenological variation even among short-lived taxa^{11,39}. Our study extends these results by showing that the predominance of plasticity over adaptation associated with temperature-related variation in phenology over space might be the norm among North American species.

The greater importance of plasticity found in this study does not contradict the well-established role of phenological adaptation in space and time³⁸ that can mediate rapid temporal shifts in phenology⁵ or facilitate ecological invasions^{6,40}. Indeed, 45% of species in our data showed evidence of adaptation-driven phenological variation along temperature gradients (Fig. 2b). It is also possible that we did not detect non-linear or patchy adaptation patterns, or that the contributions of apparent adaptation and plasticity may be different in regions underrepresented in our data (e.g., the Great Plains and prairies; Fig. S3). Crucially, we only assessed the apparent contributions of plasticity and adaptation to observed variation in flowering time over temperature gradients, so our results do not rule out the possibility that adaptation is the primary driver of phenological variation along different climatic gradients.

Still, the strong correlation between S_{space} and S_{time} has important implications for phenoclimatic research. For example, it suggests that temperature-related variation in flowering time among conspecific populations is a good proxy of responsiveness to interannual temperature variation. Therefore, space-for-time substitutions might be viable approaches to quantify plastic flowering responsiveness to temperature in North American angiosperms, for most of which we lack long-term phenological records^{26,41}.

Our results also indicate that plasticity may have generated phenological variation across a temperature range (i.e., an among-species median 90% range of 9.9 °C) exceeding the degree of warming forecasted for most regions in coming decades. However, such plastic flowering shifts over space will not necessarily be mirrored by temporal shifts within populations as warming trends continue. For example, historical temperature cues may become uncorrelated from the factors mediating the fitness consequences of phenology, rendering plastic reaction norms maladaptive^{3,10}. Plastic phenological shifts associated with warming may also be constrained by physiology⁴² or by other competing cueing mechanisms such as photoperiod or winter chilling that may be disrupted by phenological shifts associated with higher temperatures^{43–45}. These complexities highlight the need for research on the fitness consequences of recent and ongoing phenological shifts^{46,47}, and on the interrelated mechanisms underpinning associations between multiple abiotic cues (e.g., chilling, warming, photoperiod) and seasonal development beyond model systems^{45,48}.

Native climate and phenological niche mediate plasticity and adaptation across regions—Sensitivities transitioned from flowering advances under warming in spring to reduced sensitivity during summer and even flowering delays in early fall (Figs. 3, 4). These results support studies showing decreases in phenological sensitivity to temperature among species throughout the season in temperate biomes^{18,21,49,50}, and others showing delays in autumn or lengthening of the growing and flowering seasons under warming^{23,51–53}. Our study corroborates that such patterns are consistent across thousands of species and diverse climate zones and biomes in the continental United States.

Likewise, apparent adaptation throughout the season ($S_{\text{space}} - S_{\text{time}}$) typically transitioned from generating mean flowering advances to generating delays along temperature gradients. These results

mirror those reported by Delgado et al.²³, who found changes in the direction of apparent plasticity and adaptation throughout the growing season for multiple trophic levels (i.e., saprotrophs, primary producers, and primary and secondary consumers) in Eastern Europe. That changes in apparent plastic and adaptive responses to warming throughout the year might be robust across different phenophases, taxa, trophic levels, or climatic regimes may reflect shared cueing mechanisms or selective pressures for different phenological events occurring during the same seasons⁵³.

Conclusions

Our findings indicate that phenotypic plasticity is the predominant historical mechanism of spatial phenological variation across a wide range of temperature conditions in the continental United States; adaptation plays more context-specific roles. Whether and how species-level attributes such as functional traits and life history may mediate these relative contributions or whether historical responses will tend to be adaptive under non-analog climatic conditions remain open questions and promising directions for future research. Our results also outline broad correlational patterns whose verification will require direct measurements of plasticity and adaptation across species and climate regions. Our data—across many biomes and thousands of species—confirmed patterns of plastic and adaptive phenological advances in spring and delays in fall in response to warming observed in detailed empirical studies, highlighting the increasing utility of biological collections for studying plant responses to global change at vast taxonomic and spatiotemporal scales.

Materials and Methods

Phenological data

We assembled digitally available specimen records from 220 herbaria across the United States (Note S1). Species names were harmonized using the Taxonomic Name Resolution Service⁵⁴. We excluded: conspecific specimens collected within the same GPS locations and the same dates (i.e., duplicates); specimens not explicitly recorded as bearing flowers; lacking GPS coordinates, dates of collection, or species-level identification; and specimens collected outside of the United States. For subsequent analysis, we selected species represented by at least 300 specimens to ensure that our model was computationally tractable and that we had sufficient sample sizes for estimating temperature responses in space and time. The net result was a sample of 1,038,027 specimens that included 1,605 species (Fig. S3). We used day of year ('DOY') of collection of each specimen as a proxy for flowering date. Because flowering spanned year-ends for many species, we accounted for the DOY discontinuity between December 31st and January 1st using an Azimuthal correction, whereby DOYs from the year prior become negative values²⁹.

Climatic data

Temperature conditions preceding and leading up to anthesis can mediate flowering time through their effects on developmental rates of preceding phenophases or by cuing floral development and anthesis. Accordingly, we used mean surface temperatures averaged over a standard period of three months^{18,21,50,55} leading up to (and including) the mean flowering month for each species (hereafter 'TMEAN') as a predictor. For each collection site, we obtained monthly TMEAN time series (January 1901 – December 2021) at a 4-km² spatial resolution from the Parameter-elevation Regressions on Independent Slopes Model (PRISM Climate Group, Oregon State University, <http://prism.oregonstate.edu>). We characterized each collection site by its long-term mean temperature (hereafter 'TMEAN_{Normal}'), averaging observed TMEAN across all years between 1901 and 2021. Annual deviations from long-term TMEAN conditions (hereafter 'TMEAN_{Anomaly}') at each site and in each year were calculated by subtracting the TMEAN_{Normal} from the observed TMEAN conditions in the year of collection. Positive and negative TMEAN_{Anomaly} values respectively reflect warmer-than-average and colder-than-average years. TMEAN_{Normal} and TMEAN_{Anomaly} were uncorrelated irrespective of the latitudinal and elevational range spanned by a species (median $r = -0.04$), thus representing independent axes of climatic variation (Fig. S4). TMEAN_{Normal} spanned a wider temperature range than TMEAN_{Anomaly} for most species, with respective median 90% ranges of 9.9 °C and 3.7 °C (Fig. S5). Species occurring in cold climates tended to show later mean flowering dates than species occupying warmer regions (Fig. S6a); consequently, average TMEAN_{Normal} values were well above 0°C leading up to the mean flowering dates of all species in our data (Fig. S6b)

To assess how sensitivities varied across climatic gradients (see **Analyses**, below), we first characterized long-term precipitation and temperature at each site of collection using a Principal Component Analysis (PCA), with mean annual temperature normal (MAT_{Normal}), mean annual precipitation normal (PPT_{Normal}), temperature seasonality, and precipitation seasonality as input features. We obtained precipitation (hereafter 'PPT') data from PRISM and calculated PPT and temperature seasonality for each collection site as the difference between the months with the highest and lowest PPT and mean temperature normal, respectively. We made PPT seasonality proportional to local levels of precipitation by dividing differences in maximum versus minimum monthly precipitation normal by PPT_{Normal} at each site. The PCA identified 2 principal components accounting for more variance than its input features, jointly explaining 78% of observed variation. PC1 was associated with increasing PPT seasonality (36%), decreasing temperature seasonality (31%) and increasing MAT_{Normal} (28%) (Fig. S7). PC2 represented a gradient of decreasing PPT_{Normal} (74%) and increasing temperature seasonality (22%).

Analyses

Estimating flowering time sensitivity to temperature over space and time—We estimated flowering time sensitivity to TMEAN_{Normal} and TMEAN_{Anomaly} using a Bayesian mixed-effect model. The model fitted species-specific intercepts and slopes and treated them as random effects sampled from 'community-level' distributions (defined by among-species mean and standard deviation of intercepts and slopes). This hierarchical structure improved estimation of parameters by using information and estimates from

all species in the data. In turn, the Bayesian inference framework allowed for estimation of the correlations between TMEAN sensitivities over space and time and their differences for each species while propagating parameter uncertainty.

We used DOY for each observation i as a response, assuming a normal distribution with mean μ_i and species-specific standard deviation σ_{sp} :

$$DOY_i \sim N(\mu_i, \sigma_{sp}) \quad (1)$$

We modeled μ_i as a linear function of TMEAN_{Normal} (TMEAN Norm _{i}), and TMEAN_{Anomaly} (TMEAN Anom _{i}) for each observation i .

$$\mu_i = \alpha_{sp} + S_{space_{sp}} \times TMEAN\ Norm_i + S_{time_{sp}} \times TMEAN\ Anom_i \quad (2)$$

For each species sp , the model yielded intercepts representing mean flowering dates (α_{sp}), sensitivities (i.e., regression slopes) for TMEAN normal ($S_{space_{sp}}$), and sensitivities for TMEAN anomaly ($S_{time_{sp}}$).

To assess the correlation between S_{space} and S_{time} , we modeled community-level distributions for intercepts and slopes as generated by a multivariate normal distribution with a vector of hyper-means μ and a variance-covariance matrix Σ :

$$(\alpha_{sp}, S_{N_{sp}}, S_{A_{sp}}) \sim N(\mu, \Sigma) \quad (3)$$

We also calculated the difference between sensitivity types ($S_{space_{sp}} - S_{time_{sp}}$) as a derived quantity within the model, which we interpreted as the degree of apparent local adaptation in DOY observed across the TMEAN normal gradient (Fig. 1), with negative and positive values respectively indicating advances and delays in flowering DOY across warmer locations.

We used weakly informative priors, with wide, 0-centered normal distributions for intercepts, slopes, and rate parameters for exponential distributions (used to obtain species-specific variances). For the variance-covariance matrix Σ , we used a Lewandowski-Kurowicka-Joe (LKJ) Cholesky covariance prior, with $\eta = 1$ to allow for high correlations among parameters. Posterior distributions were obtained using Hamiltonian Monte Carlo (HMC) in Stan (code provided in Note S2) as implemented in R v.4.2.1 using the 'rstan' package v.2.21.2⁵⁶. We implemented a non-centered parameterization to improve sampling of the parameter space. Sampling was done using three MCMC chains with a training period of 1000 iterations

and sampling of 4000 iterations. All S_{space} , S_{time} , and $S_{\text{space}} - S_{\text{time}}$ estimates had Gelman-Rubin statistics ("R-hat") of less than 1.002, and visual examination of trace plots confirmed convergence.

Fitting the model on simulated data (Note S3), which emulated the average range of TMEAN conditions and the signal-to-noise ratio of DOY vs. TMEAN observed within species in our data, confirmed that our model could accurately recover the parameters of interest (S_{time} , S_{space} , and $S_{\text{space}} - S_{\text{time}}$) for a range of sample and effect sizes (Figs. S8–10). Moreover, we found that apparent plasticity (S_{time}) and apparent adaptation ($S_{\text{space}} - S_{\text{time}}$) could be estimated with similar degrees of precision (Fig. S11).

Because our model did not include an explicit temporal predictor, it may appear to ignore widespread trends in phenology and temperature reported in recent decades (19). However, additional simulation analyses (Note S4) showed that our model does account for temporal trends in phenology among species that experience trends in $\text{TMEAN}_{\text{Anomaly}}$ over time and are responsive to $\text{TMEAN}_{\text{Anomaly}}$ (i.e., non-zero S_{time}) (Fig. S12a). To evaluate the model's implicit assumption that trends in $\text{TMEAN}_{\text{Anomaly}}$ cause observed trends in phenology, we used the herbarium dataset to determine empirically whether observed temporal trends in $\text{TMEAN}_{\text{Anomaly}}$ and a species' S_{time} indeed explain observed trends in DOY. We recovered the same patterns observed in the simulation (Fig. S12b), suggesting that phenology and $\text{TMEAN}_{\text{Anomaly}}$ trends are causally related. Moreover, detrending DOY and $\text{TMEAN}_{\text{Anomaly}}$ prior to fitting the model did not affect our results, suggesting that omitting time as a covariate was unlikely to bias our results (Fig. S13).

Finally, we evaluated the impact on our estimates of choosing alternative reference periods to calculate $\text{TMEAN}_{\text{Normal}}$ (i.e., 1901–2020 vs. 1901–1930, 1931–1960, 1961–1990, 1991–2020) (Note S5, Figs. S14–16). These analyses confirmed that period selection was unlikely to have affected our results.

Exploring biological assumptions—Herbarium specimens rarely are collected repeatedly at the same location across years. Accordingly, we found few repeated collections over time and in close enough proximity to represent single populations. Because of this, we estimated S_{space} and S_{time} using statistical methods different from ⁹ and ²³ (Note S6). Nevertheless, the interpretation of our model relied on the same simplifying assumptions: spatial slopes reflect variation among populations along a temperature gradient, temporal slopes reflect plasticity, plasticity does not vary within and among populations, and the temporal and spatial relationships between phenology and climate are not biased by confounding factors.

We evaluated the plausibility of many of these assumptions. S_{space} likely represented phenological variation among populations because conspecific specimens were collected over vast regions spanning median 90% latitudinal and longitudinal ranges of 938 km and 1250 km, respectively. In turn, S_{time} likely reflected the effects of plasticity and not adaptation: analyses including only long-lived perennials (unlikely to show microevolutionary changes over short time periods) yielded very similar results to those presented below (Fig. S2); moreover, detrending DOY and $\text{TMEAN}_{\text{Anomaly}}$ prior to fitting the model—which

may account for temporal confounds or microevolution⁵⁷—yielded nearly identical estimates (Fig. S13). Furthermore, we generated a single estimate of S_{time} per species, thus assuming uniform plastic responses within and among populations. This assumption was supported by the observation that, for a large majority of species, S_{time} did not vary along geographic gradients of long-term TMEAN, long-term PPT, TMEAN seasonality, PPT seasonality, or the joint gradients described by PC1 and PC2 (Fig. S17). Cumulative precipitation and photoperiod are unlikely to confound S_{space} and S_{time} : accounting for cumulative PPT yielded nearly identical estimates in single-species models (Fig. S18), and an analysis of 120 species collected within geographic ranges restricted to narrower latitudinal bands ($\leq 1^\circ$)—and limited geographic variation in photoperiod—yielded results very similar to those based on the entire dataset (Fig. S19). Finally, we detected no biases in S_{space} or S_{time} due to differences in sample size among species (Fig. S20), spatial autocorrelation (Fig. S21), phylogeny (Fig. S22), non-linear phenology-temperature relationships (Fig. S23), or difference range size among species (Fig. S24).

Categorizing sensitivity patterns—To assess the prevalence of apparent plasticity and adaptation among species, we categorized each species' S_{space} versus S_{time} patterns as consistent with the effects of plasticity alone (Figs. 1a,b), adaptation alone (Figs. 1c,d), the joint effects of plasticity and adaptation (co- or counter-gradient adaptation; Figs. 1e–h), or neither. Classifications were based on the proportion of the posterior probability distribution of S_{time} and $S_{\text{space}} - S_{\text{time}}$ lying in the direction of their *maximum a posteriori* (MAP) estimate (i.e., their “probability of direction”, henceforth ‘PD’). PD is bound by 0.5 (maximum uncertainty about the effect of the predictor) and 1 (certainty of an effect in the direction of the MAP estimate). We subjectively considered apparent plasticity (S_{time}) and adaptation ($S_{\text{space}} - S_{\text{time}}$) as significant when their PD was ≥ 0.95 (Table 1). Apparent plasticity and adaptation showed similar levels of estimation uncertainty both empirically (SD = 0.87 ± 0.34 d/°C for S_{time} ; SD = 0.93 ± 0.32 d/°C for $S_{\text{space}} - S_{\text{time}}$) and in preliminary simulation analyses (Note S3), suggesting sensitivity patterns were not substantially more likely to be classified as consistent with plasticity than with adaptation (and vice versa).

Table 1—Criteria for classifying the sensitivity pattern of each species as consistent with the role of plasticity only, adaptation only, the joint effects of plasticity and adaptation in a co- or counter-gradient adaptation pattern, or neither adaptation nor plasticity. The probability that S_{time} or $S_{\text{space}} - S_{\text{time}}$ differed from 0 in the direction of its maximum a posteriori (MAP) estimate (i.e., their probability of direction) was obtained from the posterior distribution of these parameters for each species.

Biological Process**Empirical Sensitivity Pattern***Plasticity only*

1. Probability of direction for $S_{\text{time}} \geq 0.95$
2. Probability of direction for $S_{\text{space}} - S_{\text{time}} < 0.95$

Adaptation only

1. Probability of direction for $S_{\text{space}} - S_{\text{time}} \geq 0.95$
2. Probability of direction for $S_{\text{time}} < 0.95$

Plasticity and Adaptation *Co-gradient*

1. Probability of direction for $S_{\text{time}} \geq 0.95$
2. Probability of direction for $S_{\text{space}} - S_{\text{time}} \geq 0.95$
3. S_{space} and S_{time} have the same direction
4. $|S_{\text{space}}| > |S_{\text{time}}|$

Counter-gradient

1. Probability of direction for $S_{\text{time}} \geq 0.95$
2. Probability of direction for $S_{\text{space}} - S_{\text{time}} \geq 0.95$

Case 1:

1. S_{space} and S_{time} have opposite direction

Case 2:

1. S_{space} and S_{time} have the same direction
2. $|S_{\text{space}}| < |S_{\text{time}}|$

Neither

1. Probability of direction for $S_{\text{time}} < 0.95$
2. Probability of direction for $S_{\text{space}} - S_{\text{time}} < 0.95$

Plasticity and adaptation across phenological niches, local climates, and ecoregions—To assess how apparent plasticity and adaptation varied with native climate and phenological niche among species, we first calculated the mean flowering DOY and the mean coordinates along the climate gradients described by PC1 and PC2 among specimens of each species. We then fit two generalized additive models (GAMs) using S_{time} or $S_{\text{space}} - S_{\text{time}}$ as responses—assumed to be normally distributed—and a three-variable tensor-product smooth of mean flowering DOY, mean PC1, and mean PC2 as a predictor. This design allowed us to assess how native climate and phenological niche jointly determined the apparent roles of plasticity and adaptation while accounting for possible interactions and non-linearities. Because S_{time} and $S_{\text{space}} - S_{\text{time}}$ are estimated quantities, we accounted for parameter uncertainty by weighting each observation by the inverse of its posterior variance (i.e., its precision).

Additionally, we assessed the relative contributions of apparent plasticity and adaptation throughout the season within ecoregions of the contiguous United States. To do so, we identified the Level II Ecoregion—

as classified by the USA Environmental Protection Agency (EPA)^{58,59}—within which each specimen was collected. We used Level II Ecoregions because they provide sufficient ecological detail to distinguish regional floras while encompassing areas broad enough for each to capture multiple species in our data. To avoid inflating species overlap among regions or the influence of species that were rarely sampled within an ecoregion, we arbitrarily considered a species as present within an ecoregion if at least 10% of its collections occurred within it. We then retained only ecoregions represented by a minimum of 8 species. Under this scheme, the median species was classified as occurring within 2 ecoregions (range = 1–7), the median ecoregion was represented by 156 species (range = 17–956 for Atlantic Highlands and Western Cordilleras, respectively), and pairs of ecoregions shared, on average, 4% of their species (range = 0–39%; Fig. S25). Of the 120 ecoregion pairs examined, 57 shared less than 1% of species, 100 shared less than 10% of species, and 114 shared less than 20% of species.

Once species × ecoregion combinations were identified ($n = 3,570$), we fitted two GAMs including apparent plasticity (S_{time}) or apparent adaptation ($S_{\text{space}} - S_{\text{time}}$) as a response, ecoregion as a categorical predictor, mean flowering DOY as continuous predictor, and a mean flowering DOY × ecoregion spline assessing the ecoregion-specific effects of mean DOY on apparent plasticity or adaptation. Again, we accounted for parameter uncertainty by weighting each observation according to the precision of its corresponding apparent plasticity or adaptation estimate. Collection locations in different ecoregions differed substantially in their long-term climatic conditions (Fig. S26). However, we assumed no intraspecific variation in S_{time} across ecoregions an assumption partially supported by the observation that S_{time} did not tend to vary along climatic gradients within species (Fig. S16). All GAMs were implemented using the ‘mgcv’ package v.1.8-40 in R^{60,61}.

Declarations

Acknowledgments

This work was supported by the National Science Foundation through NSF DEB-1556768 (to S.J.M., I.W.P.), NSF DEB-2105932 (to S.J.M., I.W.P.), NSF DEB-2105907 (to S.R.) and NSF DEB-2105903 (to C.C.D.). T.R.P is grateful to UCSB for fellowship support in the year this manuscript was completed. We thank the many herbaria, including staff and volunteers, who collected, curated, and digitized the vast volumes of herbarium specimens leveraged for this study. We thank Ann Bishop, Devin Gamble, Cameron Hannah-Bick, David Inouye, Lisa Kim, Helen Payne, and two anonymous reviewers for comments on earlier drafts of the manuscript.

Data availability

The code and data used in this study will be publicly accessible on Dryad upon publication of the manuscript.

References

1. Elzinga, J. A. *et al.* Time after time: flowering phenology and biotic interactions. *Trends Ecol. Evol.* **22**, 432–439 (2007).
2. Bradshaw, A. D. Evolutionary Significance of Phenotypic Plasticity in Plants. in *Advances in Genetics* (eds. Caspari, E. W. & Thoday, J. M.) vol. 13 115–155 (Academic Press, 1965).
3. Gienapp, P., Teplitsky, C., Alho, J. S., Mills, J. A. & Merilä, J. Climate change and evolution: disentangling environmental and genetic responses. *Mol. Ecol.* **17**, 167–178 (2008).
4. Hoffmann, A. A. & Sgrò, C. M. Climate change and evolutionary adaptation. *Nature* **470**, 479–485 (2011).
5. Franks, S. J., Sim, S. & Weis, A. E. Rapid evolution of flowering time by an annual plant in response to a climate fluctuation. *Proc. Natl. Acad. Sci.* **104**, 1278–1282 (2007).
6. Wu, Y. & Colautti, R. I. Evidence for continent-wide convergent evolution and stasis throughout 150 y of a biological invasion. *Proc. Natl. Acad. Sci.* **119**, e2107584119 (2022).
7. Merilä, J. & Hendry, A. P. Climate change, adaptation, and phenotypic plasticity: the problem and the evidence. *Evol. Appl.* **7**, 1–14 (2014).
8. Fox, R. J., Donelson, J. M., Schunter, C., Ravasi, T. & Gaitán-Espitia, J. D. Beyond buying time: the role of plasticity in phenotypic adaptation to rapid environmental change. *Philos. Trans. R. Soc. B Biol. Sci.* **374**, 20180174 (2019).
9. Phillimore, A. B., Hadfield, J. D., Jones, O. R. & Smithers, R. J. Differences in spawning date between populations of common frog reveal local adaptation. *Proc. Natl. Acad. Sci.* **107**, 8292–8297 (2010).
10. Bonamour, S., Chevin, L.-M., Charmantier, A. & Teplitsky, C. Phenotypic plasticity in response to climate change: the importance of cue variation. *Philos. Trans. R. Soc. B Biol. Sci.* **374**, 20180178 (2019).
11. Ensing, D. J. & Eckert, C. G. Interannual variation in season length is linked to strong co-gradient plasticity of phenology in a montane annual plant. *New Phytol.* **224**, 1184–1200 (2019).
12. Stinchcombe, J. R. *et al.* A latitudinal cline in flowering time in *Arabidopsis thaliana* modulated by the flowering time gene FRIGIDA. *Proc. Natl. Acad. Sci.* **101**, 4712–4717 (2004).
13. Montague, J. L., Barrett, S. C. H. & Eckert, C. G. Re-establishment of clinal variation in flowering time among introduced populations of purple loosestrife (*Lythrum salicaria*, Lythraceae). *J. Evol. Biol.* **21**, 234–245 (2008).
14. Anderson, J. T., Inouye, D. W., McKinney, A. M., Colautti, R. I. & Mitchell-Olds, T. Phenotypic plasticity and adaptive evolution contribute to advancing flowering phenology in response to climate change. *Proc. R. Soc. B Biol. Sci.* **279**, 3843–3852 (2012).
15. Conover, D. O. & Schultz, E. T. Phenotypic similarity and the evolutionary significance of countergradient variation. *Trends Ecol. Evol.* **10**, 248–252 (1995).
16. Nylin, S. & Gotthard, K. Plasticity in Life-History Traits. *Annu. Rev. Entomol.* **43**, 63–83 (1998).
17. Fitter, A. H. & Fitter, R. S. R. Rapid Changes in Flowering Time in British Plants. *Science* **296**, 1689–1691 (2002).

18. Cook, B. I. *et al.* Sensitivity of Spring Phenology to Warming Across Temporal and Spatial Climate Gradients in Two Independent Databases. *Ecosystems* **15**, 1283–1294 (2012).
19. Lapenis, A., Henry, H., Vuille, M. & Mower, J. Climatic factors controlling plant sensitivity to warming. *Clim. Change* **122**, 723–734 (2014).
20. Zhang, H., Yuan, W., Liu, S., Dong, W. & Fu, Y. Sensitivity of flowering phenology to changing temperature in China. *J. Geophys. Res. Biogeosciences* **120**, 1658–1665 (2015).
21. Park, D. S. *et al.* Herbarium specimens reveal substantial and unexpected variation in phenological sensitivity across the eastern United States. *Philos. Trans. R. Soc. B Biol. Sci.* **374**, 20170394 (2019).
22. Prevéy, J. S. *et al.* Warming shortens flowering seasons of tundra plant communities. *Nat. Ecol. Evol.* **3**, 45–52 (2019).
23. Delgado, M. del M. *et al.* Differences in spatial versus temporal reaction norms for spring and autumn phenological events. *Proc. Natl. Acad. Sci.* **117**, 31249–31258 (2020).
24. Li, D. *et al.* Climate, urbanization, and species traits interactively drive flowering duration. *Glob. Change Biol.* **27**, 892–903 (2021).
25. Davis, C. C., Willis, C. G., Connolly, B., Kelly, C. & Ellison, A. M. Herbarium records are reliable sources of phenological change driven by climate and provide novel insights into species' phenological cueing mechanisms. *Am. J. Bot.* **102**, 1599–1609 (2015).
26. Willis, C. G. *et al.* Old Plants, New Tricks: Phenological Research Using Herbarium Specimens. *Trends Ecol. Evol.* **32**, 531–546 (2017).
27. Park, D. S., Breckheimer, I. K., Ellison, A. M., Lyra, G. M. & Davis, C. C. Phenological displacement is uncommon among sympatric angiosperms. *New Phytol.* **233**, 1466–1478 (2022).
28. Ramirez-Parada, T. H., Park, I. W. & Mazer, S. J. Herbarium specimens provide reliable estimates of phenological responses to climate at unparalleled taxonomic and spatiotemporal scales. *Ecography* **n/a**, e06173 (2022).
29. Park, I. W. & Mazer, S. J. Overlooked climate parameters best predict flowering onset: Assessing phenological models using the elastic net. *Glob. Change Biol.* **24**, 5972–5984 (2018).
30. Park, I. W., Ramirez-Parada, T. & Mazer, S. J. Advancing frost dates have reduced frost risk among most North American angiosperms since 1980. *Glob. Change Biol.* **27**, 165–176 (2021).
31. Munson, S. M. & Long, A. L. Climate drives shifts in grass reproductive phenology across the western USA. *New Phytol.* **213**, 1945–1955 (2017).
32. Kopp, C. W., Neto-Bradley, B. M., Lipsen, L. P. J., Sandhar, J. & Smith, S. Herbarium records indicate variation in bloom-time sensitivity to temperature across a geographically diverse region. *Int. J. Biometeorol.* (2020) doi:10.1007/s00484-020-01877-1.
33. Pearson, K. D., Love, N. L. R., Ramirez-Parada, T., Mazer, S. J. & Yost, J. M. Phenological trends in the California poppy (*Eschscholzia californica*): digitized specimens reveal intraspecific variation in the sensitivity of flowering date to Climate Change. *Madroño* **68**, 343–359 (2021).

34. Mazer, S. J., Love, N. L. R., Park, I. W., Ramirez-Parada, T. & Matthews, E. R. Phenological sensitivities in two *Clarkia* congeners: indirect evidence for facilitation, convergence, niche conservatism, or genetic constraints. *Madroño* **68**, 388–405 (2021).
35. Kramer, K. Phenotypic plasticity of the phenology of seven European tree species in relation to climatic warming. *Plant Cell Environ.* **18**, 93–104 (1995).
36. Levin, D. A. Flowering-time plasticity facilitates niche shifts in adjacent populations. *New Phytol.* **183**, 661–666 (2009).
37. De FRENNE, P. *et al.* Temperature effects on forest herbs assessed by warming and transplant experiments along a latitudinal gradient. *Glob. Change Biol.* **17**, 3240–3253 (2011).
38. Franks, S. J., Weber, J. J. & Aitken, S. N. Evolutionary and plastic responses to climate change in terrestrial plant populations. *Evol. Appl.* **7**, 123–139 (2014).
39. Vitasse, Y. *et al.* Elevational adaptation and plasticity in seedling phenology of temperate deciduous tree species. *Oecologia* **171**, 663–678 (2013).
40. Colautti, R. I. & Barrett, S. C. H. Rapid Adaptation to Climate Facilitates Range Expansion of an Invasive Plant. *Science* **342**, 364–366 (2013).
41. Wolkovich, E. M., Cook, B. I. & Davies, T. J. Progress towards an interdisciplinary science of plant phenology: building predictions across space, time and species diversity. *New Phytol.* **201**, 1156–1162 (2014).
42. Chown, S. *et al.* Adapting to climate change: a perspective from evolutionary physiology. *Clim. Res.* **43**, 3–15 (2010).
43. Fu, Y. H. *et al.* Declining global warming effects on the phenology of spring leaf unfolding. *Nature* **526**, 104–107 (2015).
44. Güsewell, S., Furrer, R., Gehrig, R. & Pietragalla, B. Changes in temperature sensitivity of spring phenology with recent climate warming in Switzerland are related to shifts of the pre-season. *Glob. Change Biol.* **23**, 5189–5202 (2017).
45. Wolkovich, E. M., Chamberlain, C. J., Buonaiuto, D. M., Ettinger, A. K. & Morales-Castilla, I. Integrating experiments to predict interactive cue effects on spring phenology with warming. *New Phytol.* **235**, 1719–1728 (2022).
46. Iler, A. M., CaraDonna, P. J., Forrest, J. R. K. & Post, E. Demographic Consequences of Phenological Shifts in Response to Climate Change. *Annu. Rev. Ecol. Evol. Syst.* **52**, annurev-ecolsys-011921-032939 (2021).
47. De Lisle, S. P., Mäenpää, M. I. & Svensson, E. I. Phenotypic plasticity is aligned with phenological adaptation on both micro- and macroevolutionary timescales. *Ecol. Lett.* **25**, 790–801 (2022).
48. Amasino, R. Seasonal and developmental timing of flowering. *Plant J.* **61**, 1001–1013 (2010).
49. Wolkovich, E. M. *et al.* Warming experiments underpredict plant phenological responses to climate change. *Nature* **485**, 494–497 (2012).

50. Mazer, S. J. *et al.* Flowering date of taxonomic families predicts phenological sensitivity to temperature: Implications for forecasting the effects of climate change on unstudied taxa. *Am. J. Bot.* **100**, 1381–1397 (2013).
51. Beil, I., Kreyling, J., Meyer, C., Lemcke, N. & Malyshev, A. V. Late to bed, late to rise—Warmer autumn temperatures delay spring phenology by delaying dormancy. *Glob. Change Biol.* **n/a**, (2021).
52. Zhou, Z. *et al.* Lengthened flowering season under climate warming: Evidence from manipulative experiments. *Agric. For. Meteorol.* **312**, 108713 (2022).
53. Roslin, T. *et al.* Phenological shifts of abiotic events, producers and consumers across a continent. *Nat. Clim. Change* 1–8 (2021) doi:10.1038/s41558-020-00967-7.
54. Boyle, B. *et al.* The taxonomic name resolution service: an online tool for automated standardization of plant names. *BMC Bioinformatics* **14**, 16 (2013).
55. Calinger, K. M., Queenborough, S. & Curtis, P. S. Herbarium specimens reveal the footprint of climate change on flowering trends across north-central North America. *Ecol. Lett.* **16**, 1037–1044 (2013).
56. Carpenter, B. *et al.* Stan: A Probabilistic Programming Language. *J. Stat. Softw.* **76**, (2017).
57. Iler, A. M., Inouye, D. W., Schmidt, N. M. & Høye, T. T. Detrending phenological time series improves climate–phenology analyses and reveals evidence of plasticity. *Ecology* **98**, 647–655 (2017).
58. Omernik, J. M. Ecoregions of the Conterminous United States. *Ann. Assoc. Am. Geogr.* **77**, 118–125 (1987).
59. Omernik, J. M. & Griffith, G. E. Ecoregions of the Conterminous United States: Evolution of a Hierarchical Spatial Framework. *Environ. Manage.* **54**, 1249–1266 (2014).
60. Wood, S. N. *Generalized additive models: an introduction with R.* (CRC Press/Taylor & Francis Group, 2017).
61. R Core Team. R: A language and environment for statistical computing. (2013).

Figures

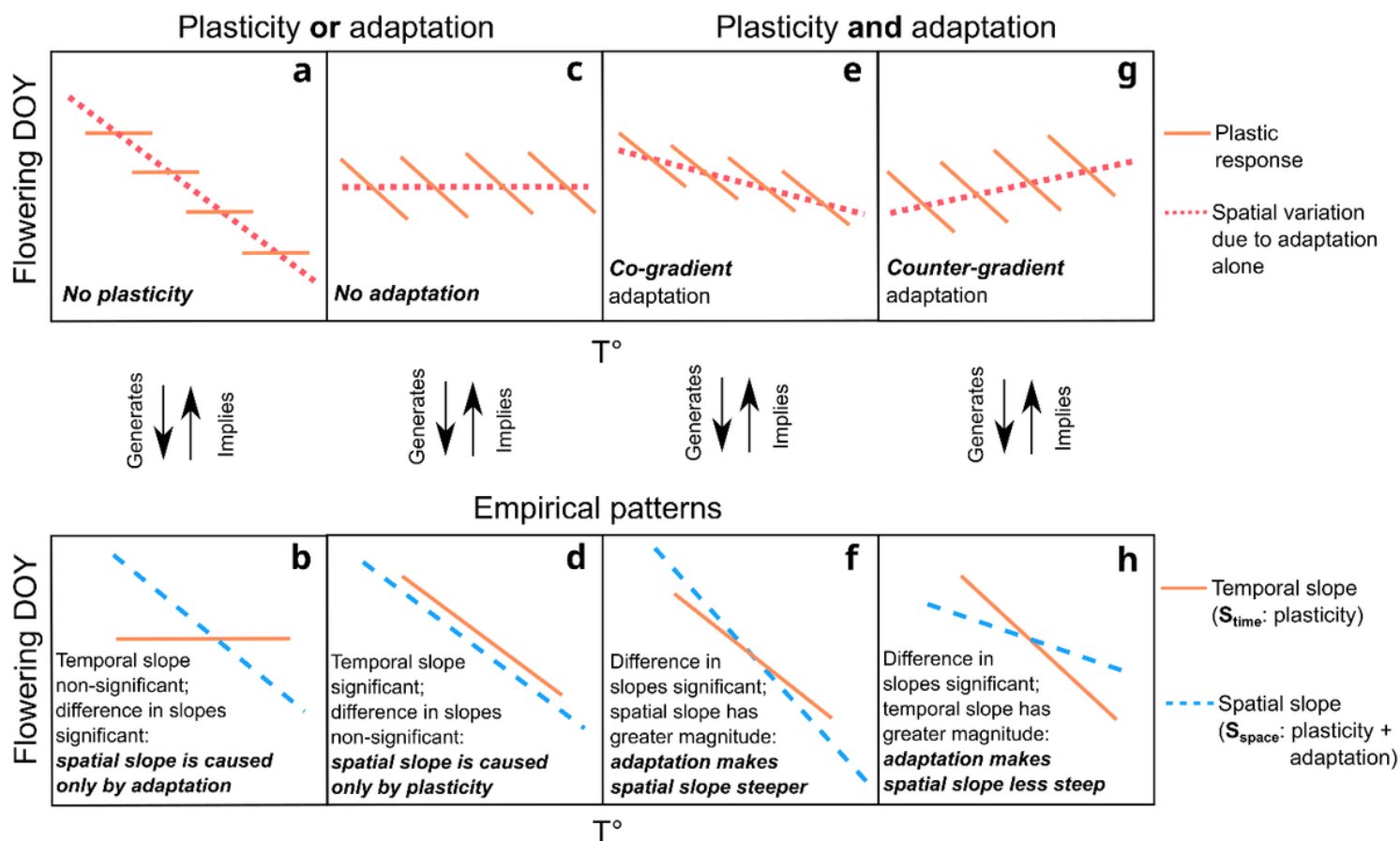


Figure 1

Diagram of four relationships between flowering time and temporal temperature variation (hereafter ‘temporal relationships;’) and spatial temperature variation (hereafter ‘spatial relationships’) that predicted by the additive effects (or lack thereof) of plasticity and adaptation along temperature gradients. **(a)** Local adaptation acting as the sole driver of flowering in time along the gradient (i.e., no phenological plasticity) should result in **(b)** a negligible temporal relationship and a biologically significant difference between temporal and spatial slopes. In contrast, **(c)** plasticity acting as the sole driver of flowering time variation along the gradient (i.e., no adaptation) should result in **(d)** a biologically significant temporal relationship and negligible differences between spatial and temporal slopes. Local adaptation and plasticity jointly influencing flowering time should result in different empirical patterns depending on the direction of their effects. **(e)** Plasticity and adaptation operating in the same direction should result in **(f)** a biologically significant temporal relationship and a spatial relationship of significantly greater magnitude. In contrast, **(g)** plasticity and adaptation operating in opposite directions should result in **(h)** a biologically significant temporal relationship and a spatial relationship of significantly lesser magnitude (or having a different sign altogether). Orange lines in **a**, **c**, **e**, and **g** illustrate phenological responses of spatially separated populations to temporal temperature variation, which spans a narrower temperature range than spatial temperature variation across the entire species range (segmented red lines). See “**Methods – Exploring Assumptions**” for an overview of the assumptions of this approach and the degree to which they were met by our data and study design.

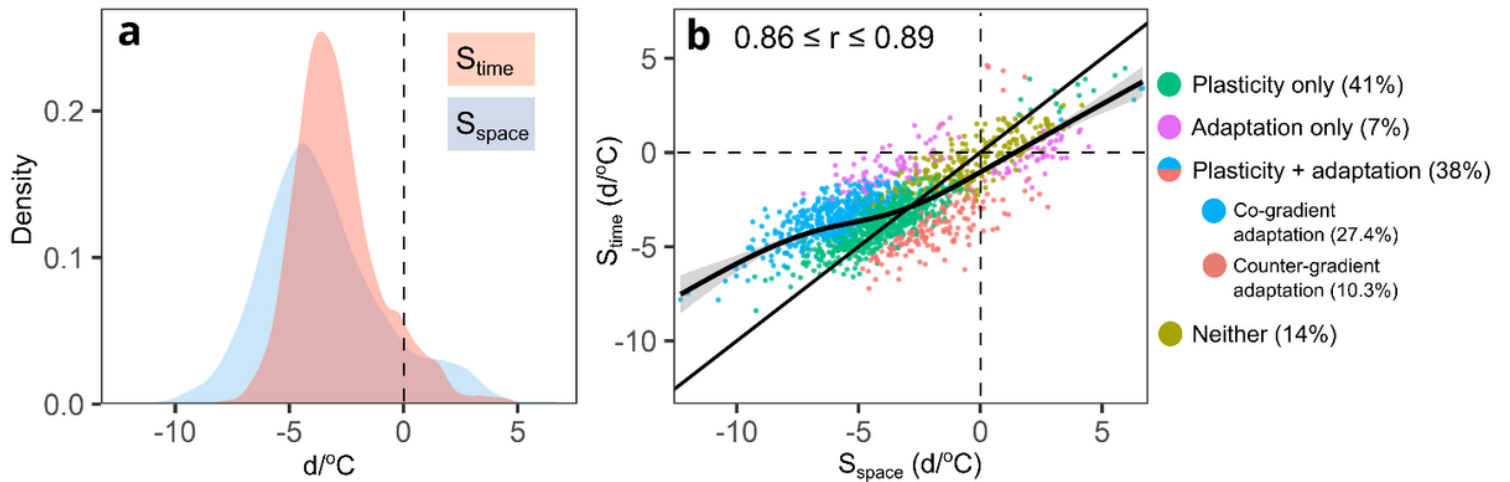


Figure 2

Distributions of, and relationship between, flowering time sensitivity to TMEAN normal (S_{space}) and to TMEAN anomaly (S_{time}) among 1,605 species in the continental United States. Shaded regions in (a) correspond to the kernel density distributions of S_{time} (red) and S_{space} (blue) among species. Each point in (b) represents a species whose x, y coordinates are given by the maximum a posteriori (MAP) estimates for S_{space} and S_{time} , respectively. Colors in (b) indicate whether sensitivity patterns were consistent with plasticity or adaptation as the sole drivers of flowering time variation along the temperature gradient, with both plasticity and adaptation in a co- or counter-gradient adaptation pattern, or neither. The straight, solid black line in (b) indicates a 1:1 relationship corresponding to perfect agreement between the two types of sensitivity, whereas the curved solid line shows the observed relationship estimated from a generalized additive model (GAM). The shaded region along the curved solid line corresponds to the standard error of the predicted value of S_{time} . The percent of species showing each pattern is shown in parentheses in the legend. The 95% credible interval for the correlation between S_{space} and S_{time} is provided as a text inset in (b).

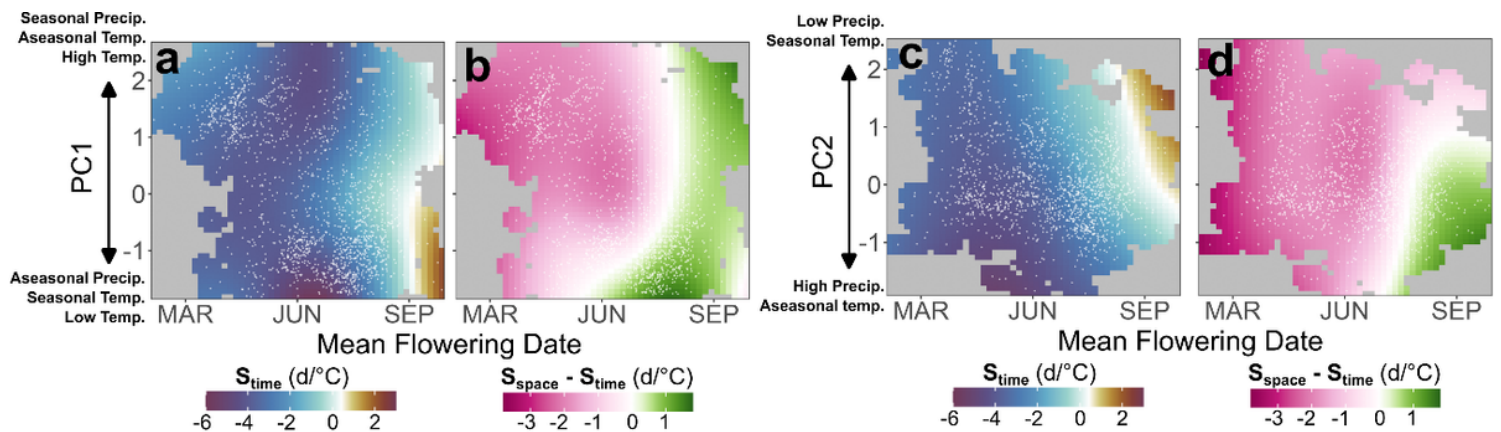


Figure 3

Variation among 1,605 flowering species in apparent plasticity (S_{time}) and apparent adaptation ($S_{\text{space}} - S_{\text{time}}$) due to differences in phenological niche and native climate. PC1 (**a, b**) represents a climate gradient of increasing precipitation seasonality, decreasing temperature seasonality, and increasing mean annual temperature, whereas PC2 (**c, d**) corresponds to a gradient of decreasing mean annual precipitation and increasing temperature seasonality. The color gradients in each panel represents the predicted magnitude of S_{time} or $S_{\text{space}} - S_{\text{time}}$ (in days/°C) for a combination of mean flowering DOY and PC1 or PC2 values. The predicted surfaces represented by the color gradients were obtained using three-variable tensor smooths in a generalized additive modelling (GAM) framework. In each panel, the value of the third variable (the one not plotted) was fixed at its mean.

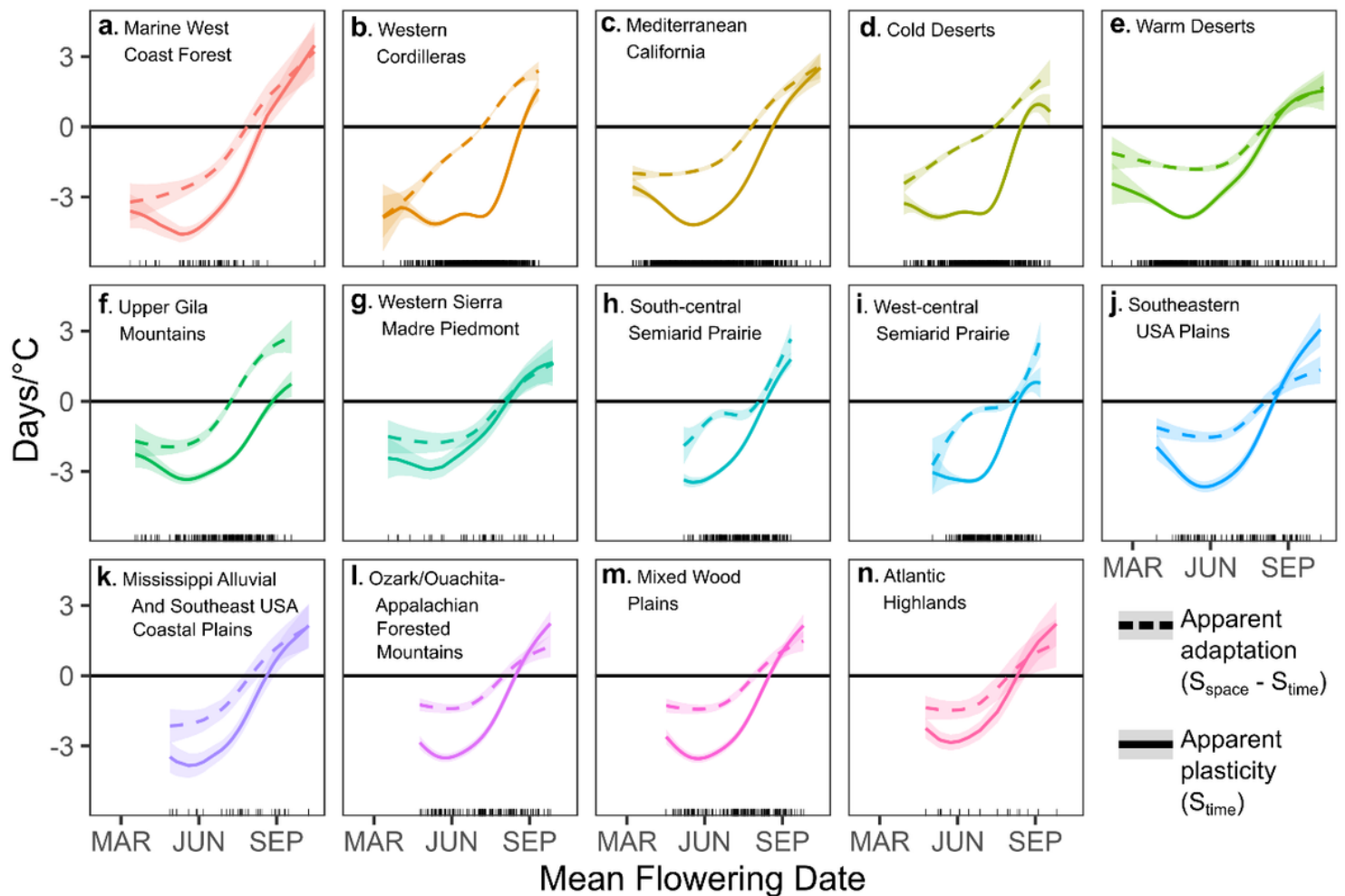


Figure 4

Relative contributions of apparent plasticity (S_{time} ; solid lines) and apparent adaptation ($S_{\text{space}} - S_{\text{time}}$; dashed lines) to phenological variation along geographic temperature gradients (S_{space}) for species with varying phenological niches and across Level II Ecoregions in the contiguous United States. Shaded regions in each panel represent the 95% confidence interval for the mean apparent plasticity or apparent adaptation among species predicted for a given mean flowering date. The predicted mean values for apparent plasticity and adaptation were obtained using generalized additive models (GAMs).

Supplementary Files

This is a list of supplementary files associated with this preprint. Click to download.

- [SupportingInformationSIRamirezParadaetal.docx](#)